Coexisting inequivalent orientations of C_{60} on Ag(001)

C. Cepek,[1,2] R. Fasel,[3] M. Sancrotti,[1,4] T. Greber,[2] and J. Osterwalder[2]
[1]*Laboratorio Nazionale TASC-INFM, AREA Science Park, Strada Statale 14 Km. 163, I-34012 Basovizza, Trieste, Italy*
[2]*Physik-Institut der Universität Zürich, CH-8057 Zürich, Switzerland*
[3]*Swiss Federal Laboratories for Materials Testing and Research, Überlandstrasse 129, CH-8600 Dübendorf, Switzerland*
[4]*INFM and Dipartimento di Matematica e Fisica, Università Cattolica del Sacro Cuore, Campus of Brescia, Via dei Musei 41, I-25121 Brescia, Italy*

(Received 30 June 2000; published 12 March 2001)

X-ray photoelectron diffraction has been used to determine the molecular orientation of C_{60} adsorbed as a monolayer on the Ag(001) surface. From an extended comparison to single scattering cluster calculations, we find the presence of two inequivalent prevailing molecular orientations of the C_{60} cage, as well as a considerable fraction of rotationally not-ordered molecules. In this system, scanning tunneling microscopy (STM) investigations have shown the presence of two differently imaged molecules that the authors proposed to originate from different bonding states [E. Giudice *et al.*, Surf. Sci. **405**, L561 (1998)]. Our analysis suggests a relation between imaging property and rotational order or not-order, while the two prevailing orientations are not distinguished by the existing STM data in this case.

DOI: 10.1103/PhysRevB.63.125406 PACS number(s): 79.60.Dp, 61.48.+c, 68.55.Jk

I. INTRODUCTION

The electronic structure and the growth mode of C_{60} molecules on different metal and semiconductor surfaces have attracted much interest in the last few years. Depending on the substrate, single layers of C_{60} molecules have been found in different geometrical arrangements and bonding states.[1] To optimize the bonding with the surface, the molecules can arrange in some preferred orientations, can become distorted, and, in some cases, induce structural instability and reconstruction of the substrate.[1,2] Therefore, an important property of these systems is the molecular orientation of the cage with respect to the surface, which is directly related to the interfacial interaction between the substrate and the molecules.

Recently, angle scanned x-ray photoelectron diffraction (XPD) has been successfully used to determine the molecular orientation of C_{60} adsorbed on different metallic surfaces.[3] In these studies, the C_{60} molecules have been found to arrange in a variety of different orientations, and the C_{60}–C_{60} interaction has been found to be an important parameter for the final bonding configuration.[4] In all the cases investigated so far, the experimental data are well explained if only one molecular orientation is taken into account (all the orientations that can be obtained by rotating the C_{60} cage around the surface normal by a symmetry angle of the substrate are equivalent). In the C_{60}/Cu(111) and C_{60}/Al(111) ordered monolayer systems, where photoelectron diffraction observed that the C_{60} cage is sitting on a hexagon, scanning tunneling microscopy (STM) was able to identify the molecular orientation of the molecules and confirmed that the majority of the molecules are arranged in the orientation found with photoelectron diffraction.[5]

Experimental indications on the possible coexistence of different cage orientations on a surface come from scanning tunneling microscopy (STM). Recently, Hou *et al.*[6] have shown by means of STM that different molecular orientations are present at the same time for C_{60} adsorbed on a semiconductor surface like Si(111)-(7×7). In other cases, where it was not possible to resolve the internal electronic structure, STM images show molecules that appear dim and molecules that appear bright. This contrast has been explained in terms of substrate reconstruction and/or electronic structure differences of molecules adsorbed on inequivalent sites.[7,8] For example, STM was not able to resolve the orientation of the molecules in the C_{60}/Pd(110) monolayer, where photoelectron diffraction found that the C_{60} cage is sitting on a pentagon–hexagon bond, but it showed that there are two different kinds of molecules (dim and bright), which were due to a substrate reconstruction.[8]

The C_{60}/Ag(001) ordered monolayer (ML) is another interesting system where STM images exhibit dim and bright molecules.[9] On Ag(001), C_{60} strongly interacts with the substrate[10] forming a $c(6\times4)$ superlattice and, in average, it is in a charge state close to -2.[11] The dim/bright contrast observed by STM has been tentatively explained by Giudice *et al.*[9] supposing that it originates from different bonding states of the C_{60} molecules. The bright molecules are arranged in many small domains of differently ordered structures, without exhibiting long-range order.[9] This behavior is not observed in films deposited and measured at temperatures lower than room temperature (RT), where all C_{60} cages appear equivalent in STM.

Here we show an extended comparison between photoelectron diffraction data and single-scattering cluster (SSC) calculations, which indicates that the ordered C_{60} monolayer on the Ag(001) surface is characterized by the presence of two inequivalent molecular orientations. It will be discussed to what extent the two different molecular orientations may be related to the two C_{60} species, as seen in STM images.

II. EXPERIMENTAL

The measurements have been performed in a modified VG ESCALAB 220 spectrometer,[12] in ultrahigh vacuum conditions with a base pressure of about 1×10^{-10} mbar. Core level spectra and XPD patterns have been obtained ex-

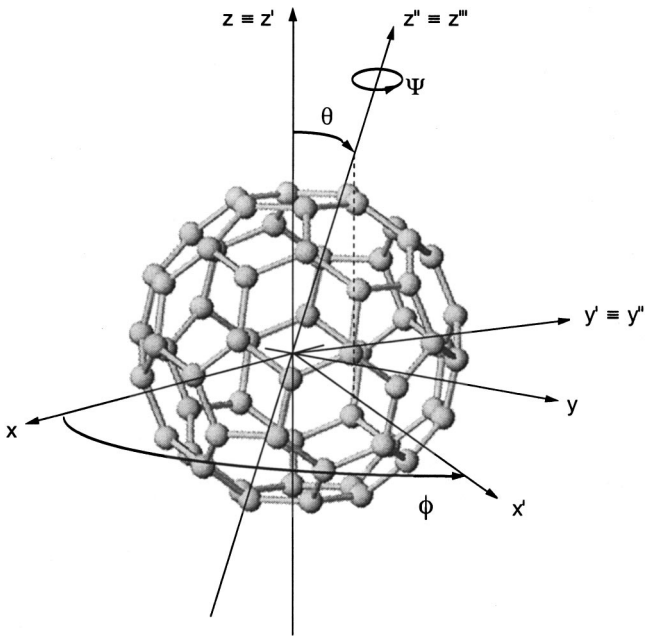

FIG. 1. Definition of the three Euler angles used to describe the C_{60} molecular orientations (see text for details).

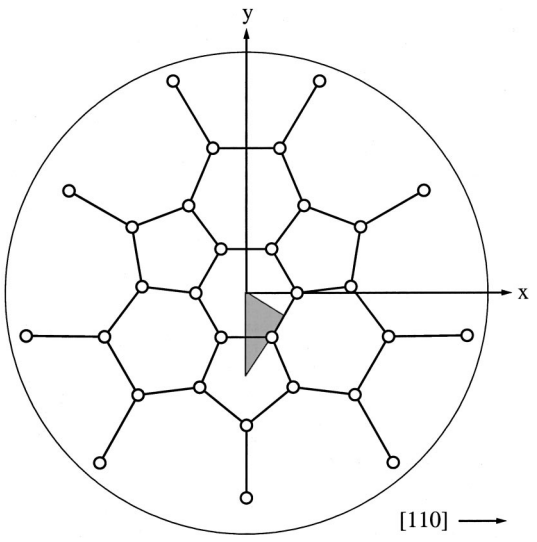

FIG. 2. Stereographic projection of the upper half of a C_{60} cage sitting on a hexagon in our *standard* orientation, where the *x* and *y* axes of Fig. 1 are also shown. The [110] direction of the substrate corresponds to the *x* axis. The shaded area contains the locations of all the inequivalent molecular axes of the C_{60} molecule.

citing the electrons by means of a conventional Mg Kα x-ray source and collecting the photoelectrons with an overall energy resolution of about 1 eV and an angular resolution of $\approx 5°$.

The XPD patterns are obtained by moving the polar and azimuthal angles of the sample with respect to the analyzer, with the angle between the x-ray source and the electron analyzer fixed to 54°.

The Ag(001) surface has been cleaned by cycles of Ar^+ sputtering ($E \approx 400$ eV) and annealing up to 800 K. Surface cleanliness and order have been checked by valence band and core level photoemission spectroscopy and low energy electron diffraction (LEED).

Pure C_{60} powder (99.9%) has been sublimated from a titanium crucible using an evaporation rate of ≈ 0.2 ML/min. The ordered ML has been obtained by evaporating the C_{60} molecules on the Ag(001) surface kept at $T \approx 600$ K. Using this preparation procedure the molecules form an ordered close packed single layer, presenting a $c(6\times 4)$ LEED pattern, where the C_{60}–C_{60} distance is ≈ 10.4 Å.[9,10]

III. CALCULATION DETAILS

All the possible C_{60} molecular orientations with respect to the surface can be described using a set of three Euler Angles (ϕ, θ, Ψ).[13] We have defined these angles, considering the rotation operations that are needed to bring a C_{60} molecule sitting on a hexagon to a particular but arbitrary orientation under consideration, as shown in Fig. 1. We indicate (*x*, *y*, *z*) as the Cartesian coordinate system of the molecule sitting on a hexagon, and for now we will call this particular orientation the *standard* orientation. The angle ϕ describes the rotation operation about the *z* axis of the molecule in the *standard* orientation, which transforms (*x*, *y*, *z*) into (x',y',$z' \equiv z$); the angle θ describes the rotation operation about the y' axis, which transforms (x',y',z') into (x'',y'',$\equiv y'$,z''); and finally, the angle Ψ describes the rotation operation about the z'' axis, which transforms (x'',y'',z'') into (x''',y''',$z''' \equiv z''$). In the following, Ψ will be called the azimuthal orientation angle. The Euler angles (ϕ, θ, Ψ) defined in this way have an immediate interpretation with respect to the orientation of the C_{60} molecular cage: the angles (ϕ, θ) define the particular molecular axis that is perpendicular to the substrate surface, and the angle Ψ defines the rotation of the molecule around this axis.

Figure 2 displays a stereographic projection of the upper half of a C_{60} cage sitting on a hexagon, in our *standard* orientation. The center of the plot corresponds to $\theta = 0°$, the border to $\theta = 90°$. Open circles indicate the carbon atoms, while the lines indicate the hexagon–hexagon and hexagon–pentagon bonds. Due to the I_h symmetry of the C_{60} molecule, only molecular axes pointing from the center of the cage through 1/12th of a hexagon or through 1/10th of an adjoining pentagon (shaded region in Fig. 2) represent inequivalent orientational configurations.[14] All the other orientations can be obtained by the proper symmetry operation from one of these inequivalent configurations.

In our *R*-factor analysis for a single molecular orientation, we have sampled the shaded region in Fig. 2, containing the location of all inequivalent molecular axes, considering a set of 112 discrete orientations (ϕ, θ). For each orientation (ϕ, θ) of the molecular axis we have then varied the azimuthal orientation Ψ of the molecule from 0° to 90° in steps of 2°, consistent with the fourfold symmetry of the Ag(001) surface. Then we have performed for each orientation single-scattering cluster calculations for individual C_{60} molecules, with no substrate present.

In the case of two coexisting inequivalent orientations, in each series of calculations, and for each of the two molecules, the shaded area in Fig. 2 was sampled using 38 dis-

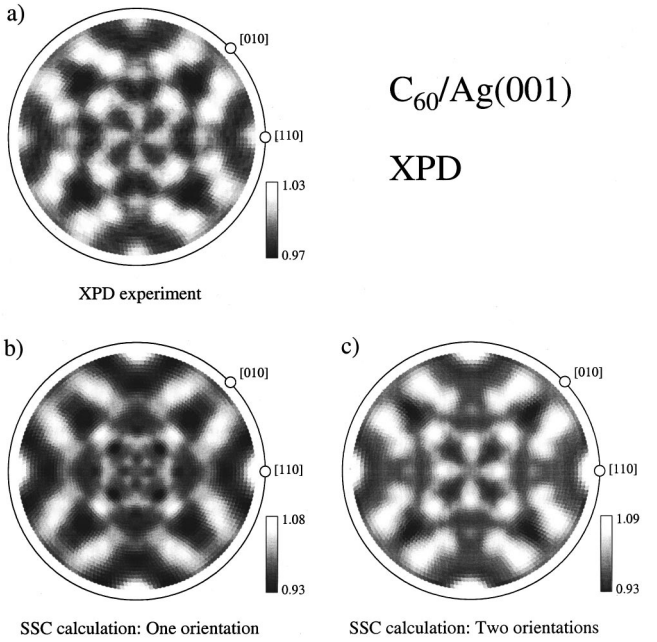

FIG. 3. Stereographic projections in a gray scale representation of (a) experimental XPD pattern of the ordered C_{60} ML on the Ag(001) surface, (b) calculated SSC pattern obtained considering one inequivalent molecular orientation, (c) calculated SSC pattern obtained considering two inequivalent molecular orientations. (See text for details.)

crete orientations of the molecular axes, and the two molecules were then independent from each other azimuthally rotated in steps of 5°. In this case, again considering the fourfold symmetry of the substrate, $38\times38\times(90°/5°)\times(90°/5°)=467\,856$ calculations were needed to obtain a first result. Then the analysis was refined around the location of the so-obtained minimum of the *R* factor. Then again we have performed for each couple of orientations single-scattering cluster calculations for C_{60} molecules, with no substrate present.

IV. RESULTS AND DISCUSSION

Figure 3(a) shows the experimental C 1*s* XPD from the ordered C_{60} monolayer grown on the Ag(001) surface. The data were measured in forward scattering condition ($E_k \approx 970$ eV) and are represented as stereographic projections in gray scale (white: maximum intensity). The center corresponds to normal emission and the border to the maximum grazing angle measured (84°). The orientation of the substrate, as determined by the XPD pattern of the Ag $3d_{5/2}$ core level, is also indicated. In order to enhance the statistical accuracy, the experimental pattern of Fig. 3(a) has been azimuthally averaged, exploiting the rotational fourfold symmetry of the substrate. This procedure did not produce any extra features with respect to the raw data. The background has been determined by linearly interpolating the photoemission signal below and above the intensity of the C 1*s* photoemission peak. Different background subtraction procedures gave similar results and do not affect the conclusions of this work.

The clear diffraction pattern indicates that a considerable

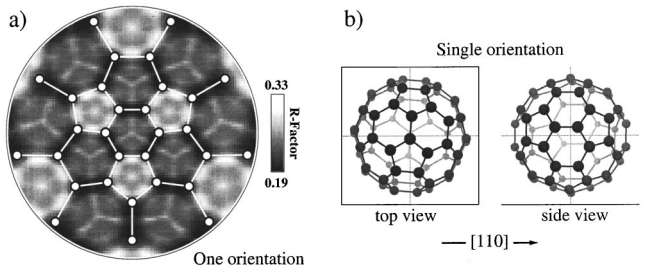

FIG. 4. (a) Stereographic representation of the *R* factor and (b) illustration of the C_{60} molecular orientation resulting from SSC calculations which take into account one inequivalent molecular orientation (see text for details). In (b) the [110] substrate direction is indicated.

fraction of C_{60} molecules are not freely rotating on the surface, and that preferred orientations of the cage are present.[3,4] In a first attempt, we tried to explain the observed pattern, taking into account one single molecular orientation with respect to the surface. The analysis was performed by minimizing the *R* factor, which was carried out by comparing the experimental diffraction pattern to single scattering cluster calculations obtained by varying the C_{60} molecular orientation (ϕ, θ, Ψ) with respect to the substrate (see Ref. 4 and Sec. II for details).

In our system, the best result is obtained with the C_{60} cage sitting close to an edge atom, and the corresponding calculated SSC pattern is shown in Fig. 3(b). A stereographic representation of the *R* factor is shown in gray scale in Fig. 4(a), which indicates also the stereographic projection of the C_{60} cage in the *standard* orientation. The filled circles indicate the carbon atoms, while the lines indicate the hexagon–hexagon and hexagon–pentagon bonds, as already described in Sec. II. Each point of the plot gives the value of the *R* factor when that particular direction [molecular axis (ϕ, θ)] of the C_{60} cage is perpendicular to the substrate surface, and the gray scale value gives the minimum value of the *R* factor from all the azimuthal orientations Ψ of the C_{60} cage. This enables us to give a simple two-dimensional representation of the *R* factor, although it depends on three parameters which are the Euler angles that describe the molecular orientation. We clearly see that the minimum of the *R* factor is obtained when the C_{60} molecules are sitting close to an edge atom ($\phi=307°$, $\theta=22.5°$, $\Psi=26°$), as shown in Fig. 4(b).

Comparing Figs. 3(a) and 3(b), it is evident, however, that the agreement between SSC calculation and experimental data is poorer than that found in the other systems investigated so far with the same method,[3,4] possibly suggesting the coexistence of several orientations. We have, therefore, performed a new series of simulations, assuming the presence of two inequivalent orientations populated with different weights (see Sec. II for details). We find that the best result is achieved when the two inequivalent orientations are almost equally populated ($45\pm15\%$ versus $55\pm15\%$). The resulting best-fit SSC calculation is shown in Fig. 3(c). In this case, there is excellent agreement with the experimental data, as confirmed by the significantly improved *R* factor (from 0.19 to 0.15). This supports the existence of two kinds of orientationally inequivalent C_{60} molecules on the surface.

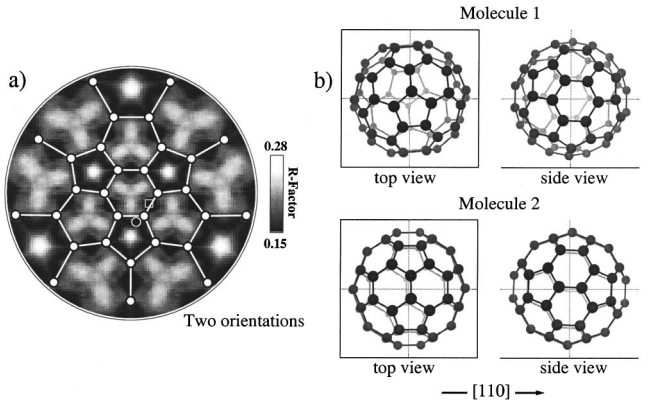

FIG. 5. (a) Stereographic representation of the *R* factor and (b) illustration of the C_{60} molecular orientations resulting from SSC calculations which take into account two inequivalent molecular orientations (see text for details). In (b) the [110] substrate direction is indicated.

A two-dimensional representation of the obtained *R* factor, similar to Fig. 4(a), is plotted in Fig. 5(a) superimposed to a stereographic projection of the C_{60} cage. We note that the *R* factor now depends on six parameters, which are the angles $(\phi_1, \theta_1, \Psi_1)$ and $(\phi_2, \theta_2, \Psi_2)$ that describe the two orientations of the molecules. In order to reduce the number of parameters, as in the case of one orientation, each point of the plot in Fig. 5(a) shows the minimum value of the *R* factor from all the azimuthal orientations of both molecules. This procedure reduces the number of parameters from six to four. Moreover, every point of the plot has an intensity that corresponds to the value of the *R* factor obtained by orienting one molecule according to the particular point considered, and the other in the position which gives the best agreement with the experimental data. This further step reduces the number of parameters from four to two and enables us to simply visualize the behavior of the *R* factor as a function of both molecular orientations. The molecular orientations corresponding to the minimum *R* factor, indicated by a circle (molecule 1: $\phi = 283°$, $\theta = 26°$, $\Psi = 38°$) and a square (molecule 2: $\phi = 324°$, $\theta = 19°$, $\Psi = 5°$) in Fig. 5(a), are schematically shown in Fig. 5(b). We note that the two orientations can be obtained by tilting a molecule sitting on an edge atom (molecular axis: $\phi = 300°$, $\theta = 23.8°$) by about 9° towards a pentagon (molecule 1: relative weight $45 \pm 15\%$) or towards a hexagon–hexagon bond (molecule 2: relative weight $55 \pm 15\%$).

The more immediate interpretation of this result is that the two inequivalent molecular orientations correspond to the two different types of molecules (bright and dim), as observed by STM[9]. According to Giudice *et al.*,[9] the C_{60} molecules, arranged in a $c(6\times4)$ ordered structure, are all sitting in equivalent sites and only a quite different electron density of states on the two kinds of molecules can explain the apparent 2 Å difference in height observed by STM. This can happen if there are two different electronic states corresponding to the two differently oriented molecules, and/or if the STM tip sees a different electron charge density on the two kinds of molecules, due to the fact that the charge is not uniformly distributed on the cage.[15] If there are two different bonding states, which depend on the C_{60} orientation, this must be reflected in the shape of the valence band and of the C 1*s* core level photoemission spectra. However, valence band[16] and high resolution core level[17] photoemission spectra, measured on this system, do not show any clear evidence of the presence of two different bonding states. In fact, the photoemission valence band spectrum of the C_{60} film, deposited at low temperature where all the C_{60} cage appear equivalent in the STM images,[9] is the same as the one measured when the two kinds of molecules are present.[16] On the other hand, the C 1*s* core level is characterized by a pronounced line shape asymmetry, an intense plasmon loss at $\approx$0.45 eV and by a full width at half-maximum of $\approx$2 eV,[17] which does not allow to resolve a possible core level shift between the two species. This indicates that only a slightly different charge transfer may exist between the two types of molecules seen in STM images, which cannot explain the huge bright/dim contrast. Moreover, we note that the two orientations that we find are very close to each other. Based on calculations for isolated molecules,[15] they are thus not expected to show significantly different densities of states to the STM tip (see Fig. 5), which would be necessary to explain the huge contrast seen in STM images. As a consequence, it is questionable to establish a direct correspondence between the two inequivalent orientations that we find and the two types of molecules seen in STM images. In fact, we recall that in the C_{60}/Pd(110) system, which shows similar bright/dim contrast in STM images, photoelectron diffraction indicates that only one orientation of the cage is present.[8] In that case, the STM contrast is due to pure topographical effects, and originates from a reconstruction of the substrate.

A simple explanation of the bright and dim molecules contrast in STM images invokes a possible reconstruction of the substrate. We propose that the adsorption site for the dim molecules is produced by a vacancy of one silver atom. As a consequence, the dim molecules sit almost in the second layer. In this case, the height difference of about 2 Å seen in STM[9] is well explained, because the distance between the first and the second layer in Ag(001) is 2.04 Å. Moreover, the low degree of long-range order between the two types of molecules seen in STM may be explained by the limited mobility of the silver ad-atoms that were removed from the first layer in forming the vacancy adsorption sites. We note, however, that from our data there is no direct evidence for a local substrate reconstruction and that this hypothesis is fully speculative. We did not observe any surface core level shift in the Ag 3*d* photoemission spectrum. However, if any, this shift is expected to be very small[18] and well below our experimental resolution ($\Delta E \approx 1$ eV). In addition, the Ag 3*d* XPD pattern measured after the deposition of the C_{60} molecules did not show any new diffraction features with respect to that of the pristine Ag(100) surface. However, also in this case, the photoelectron diffraction signal coming from the top layer atoms would be drowned by the strong contributions from all other layers. In any case, if a local substrate reconstruction takes place, we again cannot establish a direct correspondence between the bright/dim sites seen in STM images and the two molecular orientations found by XPD.

There is yet another possible model that can reconcile our XPD data with the STM images. A problem that we encounter in our simulations is that the scattering anisotropy of the best fit SSC calculations is ≈15%, more than twice the value found in the experimental data (≈6%), while in other C_{60}/metal adsorbate systems experimental and calculated anisotropies match each other well. A possible explanation is that not all the C_{60} cages are oriented in the two configurations discussed above, but that a fraction of molecules is randomly oriented with respect to the surface. In this case, the bright and dim molecules might be related to the orientationally ordered and ''disordered'' C_{60} cages. We have performed a simulation with 60% of the molecules in the orientations 1 and 2 discussed above, plus 40% of orientationally disordered molecules, which contribute to the calculated XPD pattern with a constant background. The resulting SSC pattern is obviously identical to that of Fig. 3(c), but the anisotropy is now 6%, as in the experimental data. By comparison with the STM images,[9] which show that the dim molecules are about the 60%, we can suppose that the dim molecules produce the XPD pattern, while the bright molecules are randomly oriented on the surface and cause the reduction of the anisotropy in the experimental pattern. In this case, in the ordered monolayer there are 27% molecules in the orientation 1 (45% of the ordered/dim molecules) and 33% molecules in the orientation 2 (55% of the ordered/dim molecules); and STM is not able to distinguish the different orientations.

V. CONCLUSIONS

Full-hemispherical x-ray photoelectron diffraction has been used to determine the molecular orientation of C_{60} adsorbed as a monolayer on the Ag(001) surface. From an extended comparison to single-scattering cluster calculations, we have shown that this experimental technique is able to distinguish two coexisting inequivalent orientations of C_{60} molecules adsorbed on a surface. We have discussed different models to try to understand whether the two different molecular orientations may be related to the two C_{60} species seen in STM images. The most consistent interpretation of our data and the STM images is that the dim/bright contrast is due to orientationally ordered and disordered molecules and/or to a local substrate reconstruction. In particular, we have found a correlation between the number of molecules showing dim contrast in STM images with the number of molecules showing rotational order. In both models the occurrence of the two well-discriminated molecular orientations does not seem to be relevant for explaining the dim/bright contrast.

ACKNOWLEDGMENTS

This work was partially financed under the PRA-CLASS of the INFM. C.C. would like to thank all the staff of the ESCA laboratory of the University of Zürich.

[1] See, for instance, P. Rudolf, in *Proceeding of the Xth International Winterschool on Electronic Properties of Novel Materials*, edited by H. Kuzmany, J. Fink, H. Hehring, and S. Roth (World Scientific, Singapore, 1996).

[2] J. Weaver and D. M. Poirier, in *Solid State Physics: Advances in Research and Applications*, edited by H. Ehrenreich and F. Spaepen (Academic Press, Boston, 1994), Vol. 48; T. R. Ohno, Y. Chen, S. E. Harvey, G. H. Kroll, J. H. Weaver, R. E. Haufler, and R. E. Smalley, Phys. Rev. B **44**, 13747 (1991); A. J. Maxwell, P. A. Brühwiler, D. Arvanitis, J. Hasselstöm, M. K.-J. Johansson, and N. Mårtensson, *ibid.* **57**, 7312 (1998).

[3] R. Fasel, P. Aebi, R. G. Agostino, D. Naumovic, J. Osterwalder, A. Santaniello, and L. Schlapbach, Phys. Rev. Lett. **76**, 4733 (1996).

[4] R. Fasel, R. G. Agostino, P. Aebi, and L. Schlapbach, Phys. Rev. B **60**, 4517 (1999).

[5] Y. Maruyama, K. Ohno, and Y. Kawazoe, Phys. Rev. B **52**, 2070 (1995); M. K. J. Johansson, A. J. Maxwell, S. M. Gray, P. A. Brühwiler, D. C. Mancini, L. S. O. Johansson, and N. Mårtensson, *ibid.* **54**, 13472 (1996); M. K. J. Johansson, A. J. Maxwell, S. M. Gray, P. A. Brühwiler, D. C. Mancini, and L. S. O. Johansson, Surf. Sci. **397**, 314 (1998).

[6] J. G. Hou, Y. Jinlong, W. Haiqian, L. Qunxiang, Z. Changgan, L. Hai, B. Wang, D. M. Chen, and Z. Qingshi, Phys. Rev. Lett. **83**, 3001 (1999).

[7] J. K. Gimzewski, S. Modesti, and R. R. Schlittler, Phys. Rev. Lett. **72**, 1036 (1994); P. W. Murray, M. Ø. Pedersen, E. Lægsgaard, I. Stensgaard, and F. Besenbacher, Phys. Rev. B **55**, 9360 (1997).

[8] J. Weckesser *et al.* (unpublished).

[9] E. Giudice, E. Magnano, S. Rusponi, C. Boragno, and U. Valbusa, Surf. Sci. **405**, L561 (1998); G. Costantini, S. Rusponi, E. Giudice, C. Boragno, and U. Valbusa, Carbon **37**, 727 (1999).

[10] A. Goldoni, C. Cepek, E. Magnano, A. D. Laine, S. Vandré, and M. Sancrotti, Phys. Rev. B **58**, 2228 (1998).

[11] C. Cepek, M. Sancrotti, T. Greber, and J. Osterwalder, Surf. Sci. **454–456**, 467 (2000).

[12] T. Greber, O. Raetzo, T. J. Kreutz, P. Schwaller, W. Deichmann, E. Wetli, and J. Osterwalder, Rev. Sci. Instrum. **68**, 4549 (1997).

[13] See, for instance, C. M. Lieber and Z. Zhang, Solid State Phys. **48**, 349 (1994).

[14] Y. Q. Wu, Y. L. Wu, and T. N. Raun, Commun. Theor. Phys. **27**, 297 (1997).

[15] S. Saito and A. Oshiyama, Phys. Rev. Lett. **66**, 2637 (1991).

[16] C. Cepek, L. Giovanelli, M. Sancrotti, G. Costantini, C. Boragno, and U. Valbusa, Surf. Sci. **454–456**, 766 (2000).

[17] A. Goldoni and G. Paolucci, Surf. Sci. **437**, 353 (1999).

[18] J. K. Andersen, D. Henning, M. Mathfessel, R. Nyholm, and M. Scheffler, Phys. Rev. B **50**, 17525 (1994).